

# Chemical Freezeout in Heavy Ion Collisions

Derek Teaney

*Department of Physics, Brookhaven National Laboratory, Upton, NY 11973-5000*

(Dated: February 8, 2008)

## Abstract

We construct a hadronic equation of state consistent with chemical freezeout and discuss how such an equation of state modifies the radial and elliptic flow in a hydrodynamic + hadronic cascade model of relativistic heavy ion collisions at the SPS. Incorporating chemical freezeout does not change the relation between pressure and energy density. However, it does change the relation between temperature and energy density. Consequently, when the hydrodynamic solution and freezeout are expressed in terms of energy density, chemical freezeout does not modify the hydrodynamic radial and elliptic flow velocities studied previously. Finally, we examine chemical freezeout within the hadronic cascade (RQMD). Once chemical freezeout is incorporated into the hydrodynamics, the final spectra and fireball lifetimes are insensitive to the temperature at which the switch from hydrodynamics to cascade is made. Closer inspection indicates that the pion spectrum in chemically frozen hydrodynamics is significantly cooler than in the hydro+cascade model. This difference is reflected in  $v_2(p_T)$ . We extract the freezeout hadron density in RQMD and interpret it in thermal terms; the freezeout hadron density corresponds to a freezeout temperature of  $T_f \approx 100$  MeV and  $\mu_\pi \approx 80$  MeV.

## I. INTRODUCTION

Currently, by colliding heavy ions at the Super Proton Synchrotron (SPS) and the Relativistic Heavy Ion Collider (RHIC), experimentalists [1, 2] have endeavored to create a deconfined state of quarks and gluons – the Quark Gluon Plasma (QGP). Some degree of thermalization in the heavy ion reaction is a prerequisite for QGP formation. It is an experimental fact that the ratios of the twenty or so hadron species produced in the heavy ion collision are close to the thermal ratios expected of an ideal gas of hadrons at a temperature of  $T \approx 160 - 180$  MeV [3]. It is exciting that this temperature is close to the transition temperature to the QGP,  $T_c \approx 160$  MeV. However, after accounting for finite size corrections, the hadron ratios in  $p\bar{p}$  and  $e^+e^-$  reactions are reproduced by the same thermal models used to describe heavy ion data. It seems that statistical mechanics provides a universal description of hadronization. Unlike  $p\bar{p}$  and  $e^+e^-$  reactions, the  $\sim 5000$  hadrons produced in the heavy ion collision rescatter after hadronization. Ideally, this ensemble of hadrons may be considered a hot hadronic gas; hydrodynamics then describes the subsequent evolution. With an understanding of the final hadronic expansion, the global properties of the collision can be quantified.

We first review the notion of chemical freezeout in the hadron gas [4, 5, 6, 7]. In the hadron gas, the principal hadronic reactions, e.g.  $\pi\pi \rightarrow \rho \rightarrow \pi\pi$ ,  $\pi K \rightarrow K^* \rightarrow \pi K$ ,  $\pi N \rightarrow \Delta \rightarrow \pi N$ , do not change the yields of pions, kaons, and nucleons. Nevertheless, these reactions provide a mechanism for thermalization during the hadronic evolution. Thermal equilibration times at a temperature of  $T \approx 160$  MeV are typically  $\sim 2$  fm/c [8]. In the strong interactions of light hadrons there are only three conserved currents: baryon number ( $J_B^\mu$ ), strangeness ( $J_S^\mu$ ), and isospin ( $J_I^\mu$ ). Other hadronic reactions (for instance  $\pi N \rightarrow N^*(1530) \rightarrow \Delta\pi \rightarrow N\pi\pi$ ) do change the total yield of pions, kaons and nucleons. Because of these reactions the system approaches chemical equilibrium. The yield of pions, kaons, and nucleons changes via such reactions until the Gibbs free energy reaches a minimum. However, the time scale of chemical equilibration is much longer than that of thermal equilibration; chemical equilibration times are typically  $\tau_{ch} \sim 200$  fm/c [9, 10]. Therefore in the hadron gas, there are two disparate time scales,  $\tau_{th}$  and  $\tau_{ch}$ .

In heavy ion collisions, the lifetime of the hadronic stage is approximately  $\sim 10$  fm/c, which is very short compared to  $\tau_{ch}$ , but longer than  $\tau_{th}$ . Therefore, on the time scale

of the collision, although the chemical composition is fixed at the time of hadronization, the system continues to evolve kinetically for some time until the particles breakup. The stages of the collision have been described with the following picture. First, there is chemical freezeout (hadronization). Then the hadrons evolve as a hadronic fluid until thermal freezeout (breakup). In this picture, the particles develop chemical potentials during the hadronic evolution since the total number of particles is fixed and the temperature decreases.

There is some evidence for this chemical/thermal freezeout picture. First, hadronic cascades indicate that following hadronization pions and nucleons rescatter for  $\sim 10$  fm/c. Consequently, the pion  $\langle p_T \rangle$  decreases while the nucleon  $\langle p_T \rangle$  increases. Thus, microscopic calculations indicate that pions cool and increase the transverse flow of the nucleons [11]. Second, Rapp and Shuryak have argued that a pion chemical potential can explain the anti-baryon yield at the SPS, since  $p$  and  $\bar{p}$  can be produced via the forward and backward reactions of  $\bar{p}p \leftrightarrow 5\pi$  [12]. Finally, the most compelling experimental evidence for the pion chemical potential comes from a combined analysis of spectra and HBT correlations [13]. This study indicates that the hadron density at freezeout is substantially lower than the density of a hadron gas at  $T \approx 160$  MeV. Furthermore, the pion phase space density, which can be extracted from two pion correlations, is overpopulated. An overpopulated phase space is expected from a Bose gas with a chemical potential.

Hydrodynamics has been used extensively to model heavy ion reactions. However, these hydrodynamic calculations assume thermal *and* chemical equilibrium. While thermal equilibration is at least plausible, chemical equilibration is certainly impossible. Typically a hydrodynamic simulation is run until a universal freezeout temperature  $T_f \approx 120 - 140$  MeV, which is adjusted to match the pion and nucleon spectra. Subsequently, even if the spectral shape is correct, the yields of  $\bar{p}, \Lambda, K$  for example, are typically wrong by factors of two. To account for this discrepancy, a comparison to the data is then made by rescaling the particle yields (by hand) to their value at  $T \approx 160$  MeV. Energy-momentum and number conservation are violated in this inconsistent procedure.

One approach to the problem of chemical freezeout is to stop the hydrodynamic evolution at  $T_c$  and then continue the evolution with a hadronic cascade [11, 14]. This approach incorporates chemical freezeout as chemical equilibration times are encoded into the hadronic cross sections in the cascade. Although hydro+cascade provides a comprehensive description of the heavy ion data and has been used extensively, the final spectra are sensitive to exactly

where the switch to the cascade is made [11]. Ideally, the switching temperature,  $T_{switch}$ , should be varied, with final results independent of this artificial parameter. However, the cascade conserves  $\pi, K, \Lambda \dots$  number in the dominant reactions; therefore to achieve a kind of dual description chemical freezeout must be incorporated into the hydrodynamic evolution.

This incorporation may be achieved by including additional conservation laws for  $T < T_c$ . For each conserved species  $\pi, K, \Lambda \dots$ , we have

$$\partial_\mu J_\pi^\mu = \partial_\mu J_K^\mu = \partial_\mu J_\Lambda^\mu = \dots = 0. \quad (1)$$

The Equation of State(EOS) is modified and now depends on  $n_\pi, n_K, n_\Lambda \dots$ , in addition to  $\epsilon$  and  $n_B$ . Furthermore, the relationship between energy density and temperature is dramatically different. In this work, we consistently incorporate chemical freezeout into the hydrodynamic evolution of the hydro+cascade model, H2H [14]. Similar recent efforts have been presented [15, 16]. H2H [14] and other hydrodynamic models [17, 18] have been compared extensively to available data both at the SPS and RHIC. The purpose of this work is to illustrate how chemical freezeout changes the results of these works.

Briefly, in the H2H model the initial stages of the collision are modeled with (2+1) ideal fluid dynamics, assuming Bjorken scaling in the longitudinal direction [19, 20]. The initial entropy is distributed in the transverse plane according to a Glauber model at a time,  $\tau_o = 1$  fm/c. At particular temperature,  $T_{switch}$  (which is less than the critical temperature  $T_c = 165$  MeV), the fluid is converted into hadrons via the Cooper-Frye formula [21]. The Cooper-Frye formula is appended with a theta function rejecting backward moving hadrons. Initial conditions for the hydrodynamic evolution have been chosen to match the model charged particle multiplicity and net baryon number to the experimental values at the SPS (PbPb with  $\sqrt{s} = 17$  GeV A) and RHIC (AuAu with  $\sqrt{s} = 130$  GeV A) [14].

The calculation presented here are for the SPS (PbPb with  $\sqrt{s} = 17$  GeV A) at an impact parameter of  $b=6$  fm. (A non-central impact parameter is taken in order to study elliptic flow. Final flow velocities and freezeout conditions do not change rapidly with impact parameter [14, 22].) The initial conditions (see Ref. [14] for more detail) are characterized by an entropy per baryon ratio,  $s/n_B = 42$ , and an average initial energy density,  $\langle \epsilon \rangle_{\tau_o} = 5.4$  GeV/fm<sup>3</sup>. The EOS has an 0.8 GeV/fm<sup>3</sup> latent heat and is identical (above  $T_c$ ) to the equation of state LH8 which was used previously [14]. As this work concentrates on the freezeout stages of the collision, the differences between the presented results and the

analogous calculations at RHIC are small [23]. The slightly larger baryon density at the SPS does not significantly alter the freezeout dynamics which is already meson dominated at the SPS [11, 14]

Sect. II discusses the EOS in which all the hadronic species are conserved. The hydrodynamic equations are then solved with and without the additional conservation laws and the solutions contrasted. The principal result is that the particle yields of a hydrodynamic calculation can be consistently modified (increased), provided the freezeout temperature is also modified (decreased), to keep the energy density the same. Returning to the hydro+cascade approach, in Sect. III, we vary the switching temperature to the cascade,  $T_{switch}$ . For  $115 \text{ MeV} < T_{switch} < 160 \text{ MeV}$ , the model spectra are insensitive to variations. Elliptic flow remains somewhat sensitive to the switching temperature, although the sensitivity is reduced when chemical freezeout is incorporated.

With these basic results, the freezeout conditions of the cascade RQMD are analyzed in Sect. III. At freezeout, the density of pions in the cascade is equal to the density of an ideal hadron gas with  $T_f \approx 100 \text{ MeV}$  and  $\mu_\pi \approx 80 \text{ MeV}$ . This freezeout density is universal and is independent of impact parameter, collision energy and the switching temperature,  $T_{switch}$  [11, 14]. In evaluating the extent to which the cascade reproduces the hydrodynamics in this low temperature region, we find that the hydrodynamics cools much more quickly than the cascade. This rapid cooling impacts both spectra and  $v_2(p_T)$ .

## II. IMPLEMENTING CHEMICAL FREEZEOUT IN THE EOS

In this section, we construct an EOS which incorporates chemical freezeout. (For similar constructions see [4, 10, 15, 24].) Above  $T_c$ , the EOS is identical to LH8 which was described in [14]. Only the hadronic portion of the EOS is modified.

For the purposes of this work, we consider expanding hadronic gas with only the lowest hadron multiplets. Specifically, we consider only the  $0^-$  and  $1^-$  meson octets,  $\eta'$  and  $\phi$ , the  $\frac{1}{2}^+$  baryon and anti-baryon octets and the  $\frac{3}{2}^+$  baryon and anti-baryon decuplets. The strong resonant reactions in this ensemble excite mesons and baryons from the lower hadronic multiplet to the higher multiplet and are given (up to isospin and baryon/anti-baryon symmetry) by

$$\pi\pi \rightarrow \rho \rightarrow \pi\pi \tag{2}$$

$$\pi K^+ \rightarrow K^{+*} \rightarrow \pi K^+$$

$$\pi K^- \rightarrow K^{-*} \rightarrow \pi K^-$$

$$\pi N \rightarrow \Delta \rightarrow \pi N$$

$$\pi Y \rightarrow \Sigma^* \rightarrow \pi Y$$

$$\pi \Xi \rightarrow \Xi^* \rightarrow \pi \Xi,$$

where  $Y$  denotes the hyperons  $\Lambda, \Sigma$ . These are certainly the most important reactions for the late stage of the heavy ion collision. If only these reactions and elastic collisions are included, then the system has 16 conserved currents: baryon number ( $J_B^\mu$ ), strangeness ( $J_S^\mu$ ), isospin ( $J_I^\mu$ ) and 13 other conserved numbers,  $J_{H_i}^\mu$ , where  $H_i$  runs over the hadron species,

$$\pi, \bar{N}, Y, \bar{Y}, \Xi, \bar{\Xi}, K^-, \eta, \eta', \omega, \phi, \Omega, \bar{\Omega}. \quad (3)$$

Nucleon number and  $K^+$  number are not included in the list of hadrons, but their conservation follows from the conserved hadron currents already specified and from baryon and strangeness conservation. Perhaps some of the stranger species ( $\Omega, \phi$ ) should not be included in the list of hadrons since they decouple early in the hadronic evolution. In addition,  $\omega$  does not neatly fit into the thermal/chemical freezeout picture, as its lifetime is comparable to the collision lifetime. Nevertheless, these particles are included for theoretical consistency and we have found that they do not affect the bulk properties.

With the assumption of equilibrium the hydrodynamic equations become

$$\partial_\mu T^{\mu\nu} = 0 \quad (4)$$

$$\partial_\mu (n_i u^\mu) = 0, \quad (5)$$

where  $T^{\mu\nu} = (e + p)u^\mu u^\nu - pg^{\mu\nu}$ . This set of equations, together with the assumption of smooth flow, imply entropy conservation,

$$\partial_\mu (su^\mu) = 0. \quad (6)$$

An EOS – a relation between the pressure and the energy density and number densities associated with the 16 conserved currents – is required to complete the system.

The hadronic EOS is taken as a sum of independent ideal gases over the hadrons considered. This approximation is based upon the fact that the thermodynamics of pions interacting via  $\pi\pi \rightarrow \rho \rightarrow \pi\pi$  is nearly equivalent to the thermodynamics of an ideal gas of

$\pi$ -s and  $\rho$ -s [25]. In all the ideal gas formulas, the 16 chemical potentials all appear in the combination,

$$\mu_B B + \mu_S S + \mu_I I + \sum_i \mu_{H_i} H_i, \quad (7)$$

where  $H_i$  runs over the hadron list given in Eq. 3. For instance,  $\pi^-$  has  $I = -1/2$ ,  $H_\pi = 1$ , and all other quantum numbers zero. On the other hand,  $K^{*-}$  has  $B = 0$ ,  $S = 1$ ,  $I = -1/2$ ,  $H_\pi = 1$ ,  $H_{K^-} = 1$  and all other quantum numbers zero. The EOS is a relationship between the pressure  $p$ , and the energy density  $e$ , and the number densities  $\{n_i\}$ , and is therefore a function of 1+16=17 variables.

In the heavy ion collision, only a small fraction of the total 17 variable phase space is sampled. Indeed, if at some time  $n_i/s$  is constant everywhere in space, then Eq. 6 and Eq. 4 imply that  $n_i/s$  is a constant for all later times [26, 27]. (This follows directly since  $\partial_\mu \log(s) = \partial_\mu \log(n_i) = -\partial_\mu u^\mu$ .) Thus with the assumption of entropy conservation, it is sufficient to know the EOS along the trajectory where  $n_i/s$  is constant. We now specify  $n_i/s$  and construct the hadronic EOS along this trajectory. This unique trajectory in the 17 variable phase space is called the adiabatic path below.

The ratio  $s/n_B = 42$  is fixed by the initial conditions and is chosen to reproduce the experimental proton to pion ratio [14]. The net strangeness is zero,  $n_s = 0$ . For simplicity, the net isospin is taken to be zero,  $n_I = 0$ . As discussed in the introduction, at hadronization the system is born into chemical equilibrium. Therefore at  $T_c$ ,  $n_H/s$  is taken to be its chemically equilibrated value. Now, with  $n_i/s$  a specified constant on the  $T = T_c$  hypersurface, as the system expands and cools,  $n_i/s$  remains constant. The particles develop chemical potentials to ensure this constancy. At a computational level, the procedure for constructing the EOS along the adiabatic trajectory is the following. First, at  $T = T_c$  adjust  $\mu_B, \mu_S$ , and  $\mu_I$ , until  $n_S = n_I = 0$  and  $s/n_B = 42$ . Then, calculate  $n_H/s$  at  $T_c$ . Then in small increments lower the temperature, adjust all the chemical potentials to leave  $n_i/s$  constant, and tabulate all the thermodynamic quantities (i.e, pressure, entropy, energy density) along the way.

Consider the results of this procedure. First, a few of the chemical potentials are shown as a function of the switching temperature by the thick lines in Fig. 1(a). We can derive an approximate formula for the chemical potentials as a function of  $T$ , for a collection of non-relativistic ideal gases. For non-degenerate and non-relativistic ideal gases the partial

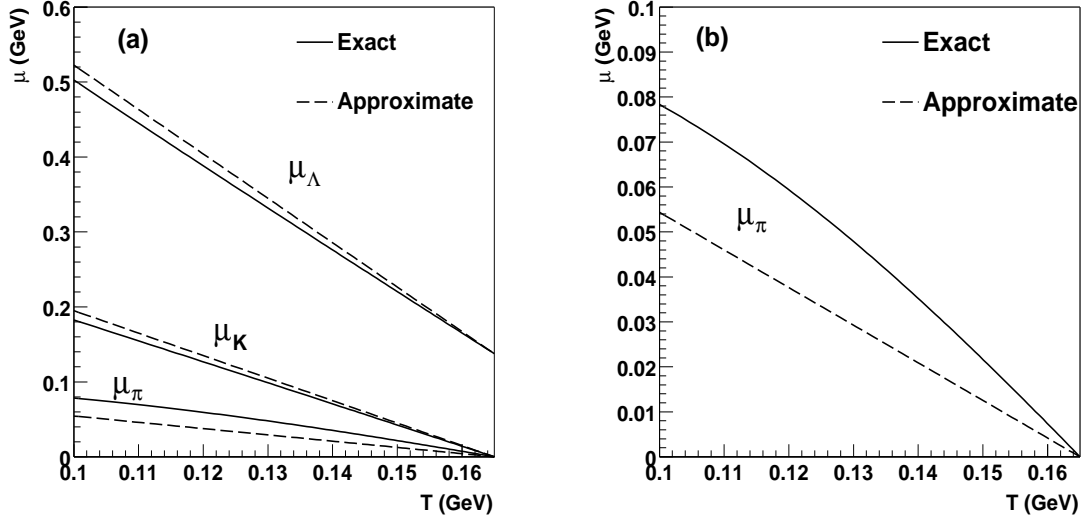


FIG. 1: Chemical potentials as a function of temperature at the SPS ( $s/n_B=42$ ) for (a)  $\pi$ ,  $K$  and  $\Lambda$  and (b)  $\pi$  only. Eq. 11 gives an approximate formula for these chemical potentials.

pressure  $p_i$ , and partial energy density  $e_i$  of the  $i$ -th species are given by,

$$p_i = n_i T \quad (8)$$

$$e_i = n_i m_i + (\text{Const}) n_i T. \quad (9)$$

Since  $T s = \sum_i \epsilon_i + p_i - \mu_i n_i$ ,

$$1 = \sum_i \frac{n_i}{s} \left( \frac{m_i + \mu_i}{T} + \text{Const} \right). \quad (10)$$

$n_i/s$  is constant below for  $T < T_c$ . To keep all the terms in parenthesis constant below  $T_c$ , we require

$$\mu_i = m_i \left( 1 - \frac{T}{T_c} \right) + \frac{T \mu_c}{T_c}, \quad (11)$$

where  $\mu_c$  is the chemical potential at the critical temperature. The approximation is shown by the dashed lines and works well for all particles except pions. Being the most important, pions are shown separately in Fig. 1(b). Thus, a pion chemical potential of nearly 80 MeV may be acquired. Similar values have been found previously [15, 24]. See [10] for a discussion of how inelastic reactions can reduce these values.

Now we return to the EOS. The energy density as a function of temperature, with and without the chemical potentials, is shown in Fig. 2. The principal observation is clear: with-



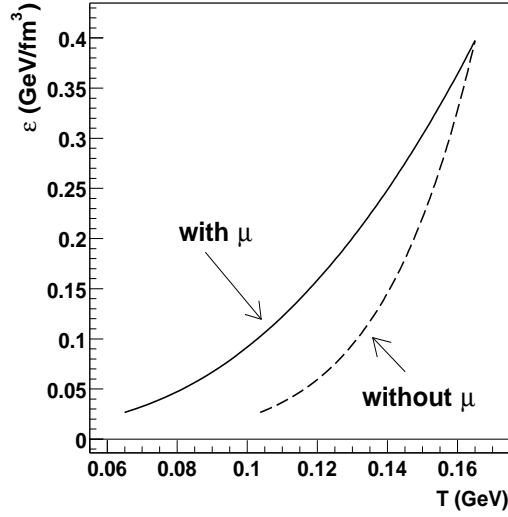


FIG. 2: The energy density as a function of temperature with and without chemical freezeout for the SPS ( $s/n_B=42$ ).

out chemical freezeout the energy density drops very rapidly as a function of temperature, since the total number of particles drops. For later discussion, the temperature is tabulated as a function of energy density with and without chemical potentials, in Table I. However, to find the hydrodynamic solution the most important quantity is not the relationship between energy density and temperature, but the relation between the energy density and pressure – the EOS. Fig. 3 shows the pressure, the squared sound speed  $c_s^2$ , and the entropy density versus the energy density along the adiabatic path. Along the adiabatic path, these quantities are all related because

$$\left(\frac{dp}{de}\right)_{\{n_i/s\}} \equiv c_s^2 \quad (12)$$

$$\left(\frac{ds}{de}\right)_{\{n_i/s\}} = \frac{s}{p + e}. \quad (13)$$

(The second relation follows by noting that  $\left(\frac{ds}{de}\right)_{n_i/s} = \left(\frac{ds}{de}\right)_{n_i} + \left(\frac{ds}{dn_i}\right)_e \frac{n_i}{s} \left(\frac{ds}{de}\right)_{n_i/s}$ , solving for  $\left(\frac{ds}{de}\right)_{n_i/s}$  and using thermodynamic identities). Unlike energy density versus temperature, pressure is scarcely modified by the chemical potentials. Differentiating the pressure, we see that  $c_s^2$  is reduced somewhat at low temperatures when chemical freezeout is incorporated. Integrating to find the entropy, we see that the entropy as a function of energy is nearly identical with and without chemical freezeout.

Energy Density ( $\text{GeV}/\text{fm}^3$ )	T(MeV) with $\mu_\pi > 0$	T(MeV) with $\mu_\pi = 0$
0.364	160	163
0.249	140	153
0.158	120	142
0.122	110	135
0.091	100	129
0.067	90	122
0.047	80	115

TABLE I: Temperature versus energy density, with and without chemical freezeout at the SPS ( $s/n_B = 42$ ).

From the point of view of dynamics, this means that the hydrodynamic solutions, with and without chemical freezeout, are nearly the same when expressed as a function of energy density. The flow velocities on a freezeout surface of constant energy density are independent of whether or not chemical potentials are included. However, the temperature on that freezeout surface depends dramatically on chemical freezeout, as can be seen from Table I. To make this point clear, the hydrodynamic solutions are illustrated in Fig. 4 with and without chemical potentials. The solutions are similar; the small differences can be traced to small differences in the speed of sound.

Often in hydrodynamic simulations not incorporating chemical freezeout, the freezeout surface  $T \approx 130$  MeV is taken [17, 18]. Using Table I, this roughly corresponds to a temperature of  $T \approx 100$  MeV. Although this temperature seems low, it is not out of keeping with the phenomenological freezeout temperatures extracted from thermal fits to radial [28] and recent elliptic flow data [29]. The extent to which this low freezeout temperature is seen in a hadronic cascade is addressed in the next section.

### III. RQMD AND CHEMICAL FREEZEOUT

Returning to hydro+cascade, we can study the extent to which chemically hydrodynamics reproduces the dynamic response of the cascade. An important observation is that with the assumption of chemical equilibrium, the hydrodynamics is independent of the dominant

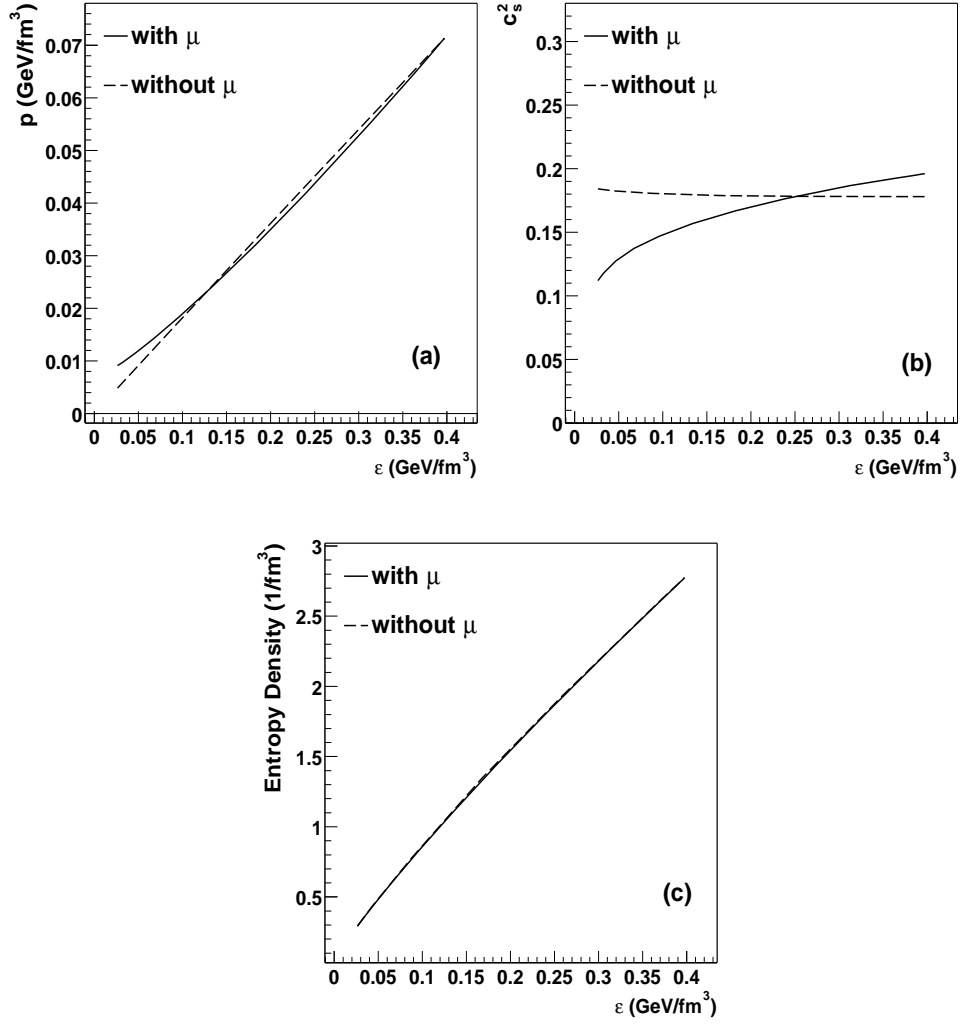


FIG. 3: The (a) pressure, (b) sound speed squared and (c) entropy density as functions of the energy density with and without chemical freezeout at the SPS ( $s/n_B=42$ ). The analogous curves at RHIC are only slightly different.

reactions in the cascade. With chemical freezeout, reactions such as  $\pi N \rightarrow \Delta \rightarrow \pi N$ , are encoded into the conservation laws and ultimately into the chemical potentials which affect the spectra. Baryons are accelerated only by reducing the kinetic energy of the pions. In a hydrodynamic language, the flow velocity is increased only by rapidly decreasing the temperature.

One of the problems with the hydro+cascade approach [11] is the sensitivity to the switching temperature. To make a smooth transition from hydrodynamics into the cascade,

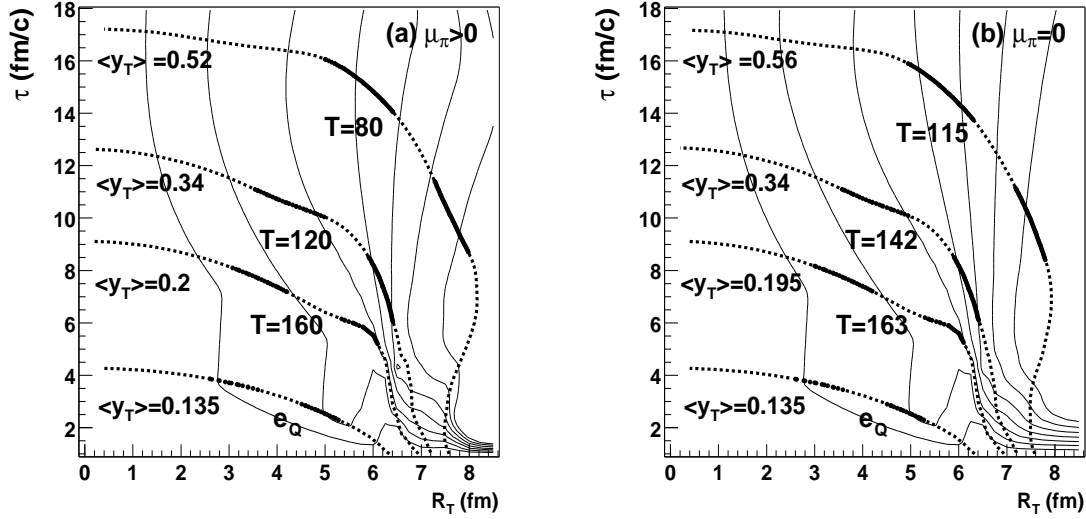


FIG. 4: The hydrodynamic solution (a) with and (b) without chemical freezeout at the SPS (PbPb,  $\sqrt{s}=17$  GeV A,  $b=0$  fm,  $s/n_B=42$ ). The thick arcs show contours of constant energy density. The first contour indicates the start of the mixed phase,  $e_Q$ . The next three contours indicate energy densities corresponding to temperatures (a)  $T = 160, 120, 80$  MeV with chemical freezeout and (b)  $T=163, 142, 115$  MeV without chemical freezeout, see Table I. The thin lines show contours of constant transverse fluid rapidity,  $y_T = 0.1, 0.2, \dots, 0.7$ . Walking along the thick arcs, the arc is divided into solid and dotted segments. 20% of the total entropy passing through the arc passes through each segment.  $\langle y_T \rangle$  denotes the mean transverse rapidity (weighted with entropy) on the arc.

the same conservation laws have to be implemented in both approaches. In Fig. 5, we adjust the switching temperature from  $T_{switch} = 160$  MeV to  $T_{switch} = 117$  MeV, and compare spectra in which chemical freezeout is incorporated,  $\mu_\pi > 0$ , to spectra in which chemical freezeout is not incorporated,  $\mu_\pi = 0$ . Ideally, the spectra should be insensitive to  $T_{switch}$ .

First, notice that if chemical freezeout is not incorporated the yields of  $K$  and  $\bar{p}$  are reduced by factors of  $e^{-\frac{M_K}{T} - \frac{M_K}{T_c}}$  and  $e^{-\frac{M_N}{T} - \frac{M_N}{T_c}}$ , or 3 and 7 for temperatures of  $T \approx 120$  MeV. Furthermore, the final flow is too strong, since both the mass energy and the kinetic energy are converted into flow. Second, notice that once chemical freezeout is incorporated, the sensitivity to the switching temperature is small. This is because the freezeout energy density is higher; therefore it is “as if” the freezeout temperature were higher. Close inspection

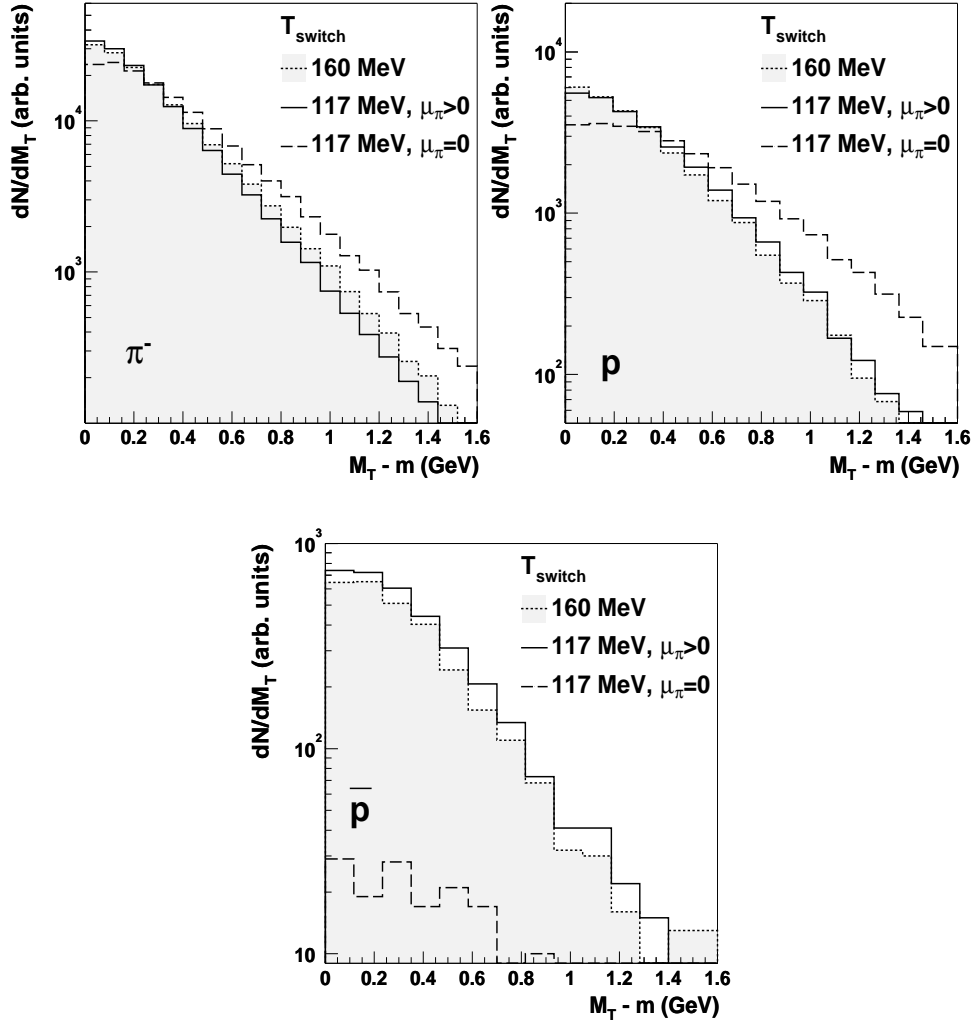


FIG. 5: Sensitivity of particle spectra at the SPS (PbPb,  $\sqrt{s}=17$  GeV A,  $b=6$  fm,  $s/n_B=42$ ) to  $T_{switch}$  with chemical freezeout,  $\mu_\pi > 0$  and without,  $\mu_\pi = 0$ . The spectra are for  $\pi^-$ ,  $p$ , and  $\bar{p}$ . The filled histograms are  $T_{switch} = 160$ . The other curves are for  $T_{switch} = 117$ .

tion of the pion spectrum shows that the final spectrum with chemical freezeout is too cool relative to the Hydro+cascade model. This rapid cooling will be addressed below.

A naive explanation for the insensitivity to  $T_{switch}$  is that the decrease in temperature is compensated by flow. Fig. 6 studies this explanation in detail. Hadronic rescattering increases the mean  $M_T$  of the nucleons while slightly decreasing the mean  $M_T$  of the pions. Although these general trends are reproduced by the hydrodynamics, with the hydrodynamics the pion cooling is too rapid and the nucleon acceleration is slightly too large. These

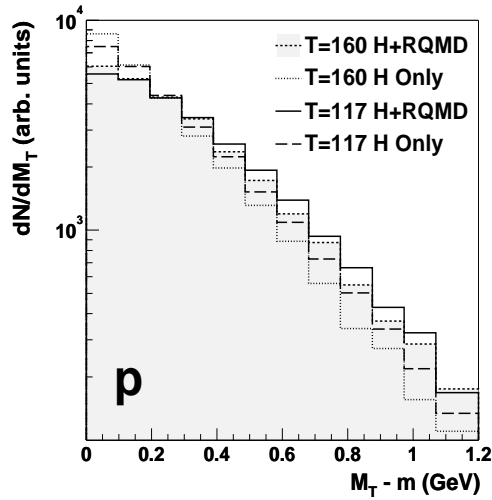


FIG. 6: The effect of hadronic scattering on the proton spectrum at the SPS (PbPb,  $\sqrt{s}=17$  GeV A, b=6 fm,  $s/n_B=42$ ) with and without chemical freezeout. The temperature  $T_{switch}$ , where the switch from hydro to cascade made is given in the figure. H(ydro)+RQMD denotes the spectra with subsequent hadronic rescattering in the cascade. H(ydro) Only denotes a spectrum in which only resonance decays but no rescattering have been accounted for.

facts may be gleaned from a very close inspection of the four curves in Fig. 6. However, the differences are all small and it is difficult to tell the difference between chemically frozen hydrodynamics and free streaming from spectra alone.

Instead of spectra, we study the elliptic flow when chemical potentials are included. Fig. 7 shows the sensitivity of elliptic flow to  $T_{switch}$ . The elliptic flow remains fairly sensitive to the switching surface and increases by 25% as the switching temperature is lowered. The hydrodynamic contribution increases while the RQMD contribution decreases as  $T_{switch}$  is lowered. The fact that the Hydro+RQMD curve is flatter than the Hydro Only curve indicates that hydro+cascade model is partially successful.

Additional information is gained with Fig. 8, which examines the elliptic flow spectrum,  $v_2(p_T)$ . The rapid cooling of the hydrodynamic response with chemical freezeout ( $T=117$   $\mu_\pi > 0$ , Hydro+RQMD) is seen as an increase in elliptic flow at modest  $p_T$ , relative to the normal curves ( $T=160$  Hydro+RQMD). By comparing the  $T = 160$  MeV Hydro Only and Hydro+RQMD points, we see that in the cascade the pions cool only slightly. Nevertheless, the general trend is the same for both the hydro with chemical freezeout and the cascade

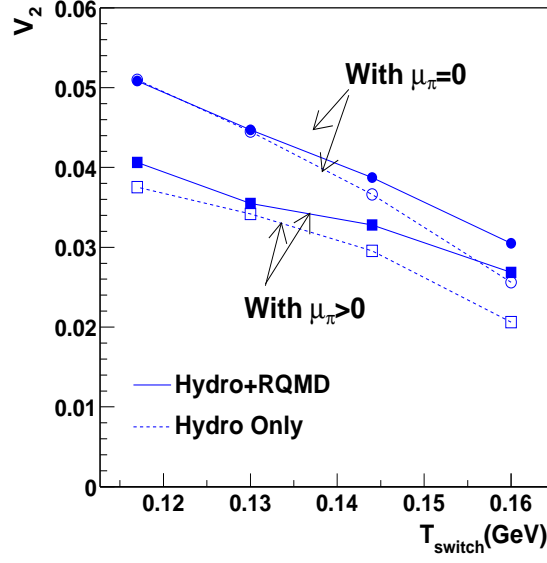


FIG. 7:  $v_2$  of pions at the SPS (PbPb,  $\sqrt{s}=17$  GeV A,  $b=6$  fm,  $s/n_B=42$ ) as a function of  $T_{switch}$  with chemical freezeout,  $\mu_\pi > 0$ , and without,  $\mu_\pi = 0$

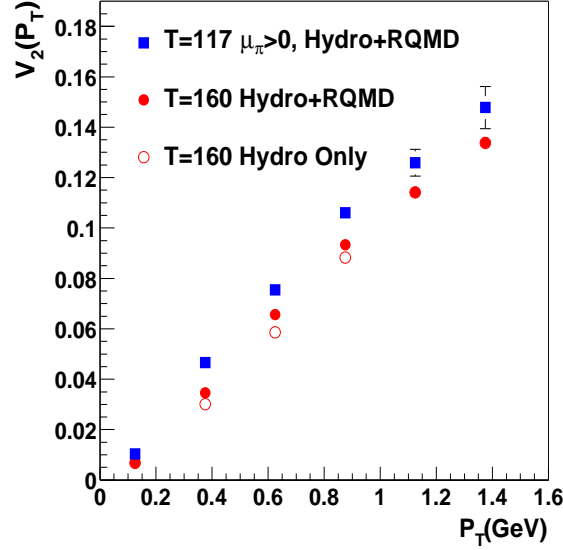


FIG. 8: The elliptic flow spectrum of pions at the SPS (PbPb,  $\sqrt{s}=17$  GeV A,  $b=6$  fm,  $s/n_B=42$ ) as a function of  $T_{switch}$  with chemical freezeout  $\mu_\pi > 0$ , and without,  $\mu_\pi = 0$ .

with chemical freezeout.

We now turn to the distribution of pions at freezeout. The density of pions at freezeout is approximately constant as a function of impact parameter and beam energy [14]. Now we interpret this density in thermal terms. In the cascade, the density of pions at freezeout is the same as the density of pions in a hadron gas with  $T \approx 110$  MeV and  $\mu_\pi \approx 70$  MeV. Notice Fig. 9, which shows the mean emission time as the switching temperature is lowered. As with the spectra, the mean emission time after cascading is insensitive to the switching temperature. The system of hadrons introduced into the cascade expands until the density reaches a certain value and subsequently breaks up. Since the number of hadrons is conserved during the hydrodynamic evolution, the final breakup does not depend on where the hydrodynamics is stopped and where the cascade begins.

We now try to measure the RQMD pion density at freezeout. The cascade does not have a freezeout surface, as is normally assumed in an idealized hydro picture. Rather, particles are emitted per unit time and volume, i.e.  $\frac{dN}{\tau d\eta dx dy d\tau}$ . We define the freezeout density in the transverse plane as

$$n_\pi^{RQMD} \equiv \frac{1}{\pi R_o^2} \int_{\sqrt{x^2+y^2} < R_o} dx dy d\tau \frac{dN}{\tau d\eta dx dy d\tau}, \quad (14)$$

where  $R_o$  is taken to be 3 fm. This density,  $n_\pi^{RQMD}$ , with and without hadronic rescattering is shown in Fig. 10. Of course, without rescattering, the density of pions should reflect the density of pions on the freezeout surface. With the EOS used in this work, this number density is simply the zero-th component of  $J_{H\pi}^\mu$  or

$$J_{H\pi}^0 = n_\pi + 2n_\rho + n_\Delta \dots \quad (15)$$

This thermal density of pions is also shown in Fig. 10 and gives a reasonable description of the Hydro Only points. When rescattering is included, the density decreases until a constant value  $\approx 0.1 \text{ fm}^3$ , is reached. Comparing the thermal model curves to the Hydro+RQMD points, we see that the freezeout densities are equal for  $T \approx 100-110$  MeV and  $\mu_\pi \approx 80$  MeV. Although this temperature is low, it is not out of keeping with the numbers extracted from hydrodynamic fits to the data [28, 29].



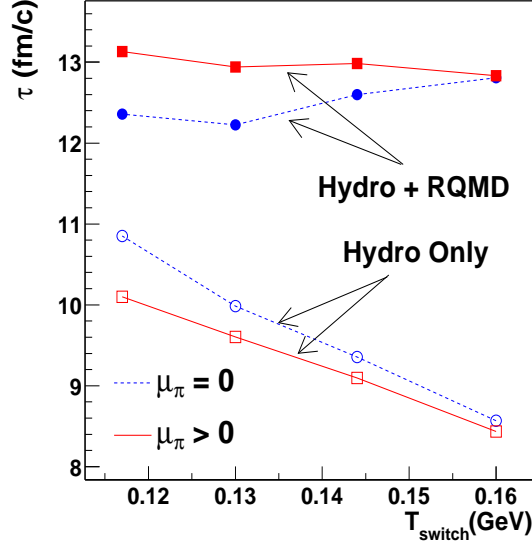


FIG. 9: The mean emission time  $\langle \tau \rangle$  at the SPS (PbPb,  $\sqrt{s}=17$  GeV A,  $b=6$  fm,  $s/n_B=42$ ) as a function of  $T_{switch}$  with chemical freezeout  $\mu_\pi > 0$ , and without chemical freezeout,  $\mu_\pi = 0$ .

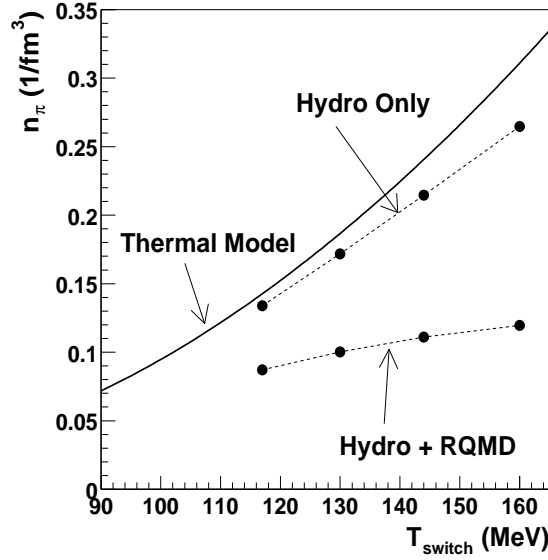


FIG. 10: The pion density at freezeout in RQMD (see Eq. 14) as a function of  $T_{switch}$  at the SPS (PbPb,  $\sqrt{s}=17$  GeV A,  $b=6$  fm,  $s/n_B=42$ ). The Thermal Model curves indicate the density of pion number (see Eq. 15) in a hadron gas, i.e.  $n_\pi + 2n_\rho + \dots$ .

#### IV. SUMMARY OF CHEMICAL FREEZEOUT

We have constructed an EOS consistent with chemical freezeout. The relationship between pressure and energy density is approximately the same as the standard EOS. However, these two EOS exhibit dramatically different relationships between energy density and temperature. At a practical level, this means that the results from a hydrodynamic calculation without chemical freezeout may be consistently converted to a calculation with chemical freezeout by simultaneously adjusting the yields and the temperature to keep the energy density constant. Table I gives the required conversion factors.

We used this chemically consistent EOS to study the hydrodynamic + hadronic cascade model, H2H [14]. Since, chemical freezeout is incorporated via the hadronic cross sections into the cascade, the same conservation laws are implemented in both the hydrodynamics and the cascade. With this congruence, we examined the model sensitivity to the switching temperature from hydro to cascade,  $T_{switch}$ . The spectra are insensitive to the switching temperature for  $120 \text{ MeV} < T_{switch} < 160 \text{ MeV}$ . On the other hand, elliptic flow at the SPS remains mildly sensitive to  $T_{switch}$  even when chemical freezeout is incorporated. The insensitivity of the model's results to  $T_{switch}$  partially validates the hydro+cascade approach.

An important feature of a chemically frozen EOS is that the principal reactions in the cascade, e.g.  $\pi N \rightarrow \Delta \rightarrow \pi N$ , are encoded into the hydrodynamics through the chemical potentials. Thus, in the cascade, the nucleons are accelerated only by reducing the kinetic energy of the pions. With a chemically frozen EOS, this qualitative feature is reproduced by the hydrodynamics. However, as might be expected, the cooling and attendant acceleration are larger in the hydrodynamics than in the cascade. When the cascade is replaced with the hydrodynamics, the pion spectrum is slightly steeper while the nucleon spectrum is slightly flatter. Pion cooling may also be seen with  $v_2(p_T)$ . Here again, the small changes in  $v_2(p_T)$  due to hadronic rescattering are strongly magnified by the hydrodynamics with chemical freezeout.

By incorporating chemical freezeout, many of the qualitative features of the cascade's evolution are reproduced with the hydrodynamics (see [30] for further investigations of this point). Thus, a thermal interpretation of the cascade's response is partially justified. Within RQMD, we find the density of pions at freezeout to be  $n_\pi \approx 0.12 \text{ fm}^{-3}$ , which corresponds to  $T \approx 110 \text{ MeV}$  and  $\mu_\pi \approx 70 \text{ MeV}$  in thermal terms. Precisely these parameters have been

extracted from thermal fits to hadronic data. Therefore, an understanding of the properties of a chemically frozen hadronic gas helps to bridge the cascade and thermal descriptions of the final stages of the heavy ion collision.

## V. ACKNOWLEDGMENTS

I thank Edward Shuryak for continued support.

## REFERENCES

- [1] Quark Matter 1999, Nucl. Phys. **A661**(1999).
- [2] Quark Matter 2001, Nucl. Phys. **A698** (2002).
- [3] P. Braun-Munzinger, J. Stachel, J.P. Wessels, N. Xu, Phys. Lett **B344**, 43 (1995); F. Becattini, M. Gadzdicki and J. Sollfrank, Eur. Phys. J. **C5**, 143 (1998); P. Braun-Munzinger, D. Magestro, K. Redlich, J. Stachel, Phys. Lett. **B518** 41 (2001); J. Cleymans and K. Redlich, Phys. Rev. **C59**, 354 (1999) ; J. Cleymans, H. Oeschler and K. Redlich, Phys. Rev.**C59**, 1663 (1999) ;
- [4] H. Bebie, P. Gerber, J.L. Goity, and H. Leutwyler, Nucl. Phys. **B378**, 95 (1992).
- [5] E. Shuryak, Phys. Lett **B207**, 345(1988); Phys. Rev. **D42**, 1764 (1990).
- [6] P. Gerber, H. Leutwyler and J.L. Goity, Phys. Lett. **B378**, 513 (1990).
- [7] S. Gavin and V. Ruuskanen, Phys. Lett. **B262**, 326 (1991); S. Gavin, Nucl. Phys. **B351**, 561 (1991).
- [8] M. Prakash, M. Prakash, R. Venugopalan, G. Welke, Phys. Rept. **227**, 321 (1993).
- [9] C. Song and V. Koch, Phys. Rev. **C55**, 3026 (1997).
- [10] S. Pratt and K. Haglin. Phys. Rev. **C59**, 3304(1999).
- [11] S. Bass and A. Dumitru, Phys. Rev. **C61**, 064909 (2000).
- [12] R. Rapp and E.V. Shuryak, Phys. Rev. Lett. **86**, 2980 (2001).
- [13] D. Ferenc, U. Heinz, B. Tomasik, U.A. Wiedemann, J.G. Cramer, Phys. Lett. **B457**, 347 (1999).
- [14] D. Teaney, J. Lauret, and E.V. Shuryak, Phys. Rev. Lett. **86**, 4783 (2001); D. Teaney, J. Lauret, and E.V. Shuryak, nucl-th/0110037.
- [15] N. Arbex, F. Grassi, Y. Hama, and O. Socolowski Jr., nucl-th/0102056.

- [16] T. Hirano and K. Tsuda, nucl-th/0202190.
- [17] P.F. Kolb, P.Huovinen, U. Heinz, H. Heiselberg, Phys. Lett **B500**, 232 (2001); P. Huovinen, P.F. Kolb, U. Heinz, H. Heiselberg, Phys. Lett **B503**, 58 (2001).
- [18] T. Hirano, Phys. Rev. **C65**, 011901 (2002); T. Hirano, Phys. Rev. Lett. **86**, 2754 (2001).
- [19] J.D. Bjorken, Phys. Rev. **D27**, 140 (1983).
- [20] J.-Y. Ollitrault, Phys. Rev. **D46**, 229 (1992).
- [21] F. Cooper and G. Frye, Phys. Rev. **D10**, 186 (1974); F. Cooper, G. Frye, E. Schonberg, Phys. Rev. **D11**, 192 (1975).
- [22] P.F. Kolb, U. Heinz, P. Huovinen, K.J. Eskola, K. Tuominen, Nucl. Phys. **A696**, 197 (2001).
- [23] D. Teaney, Ph.D. Thesis, State University of New York at Stony Brook (2001).
- [24] R. Rapp and J. Wambach, Eur. Phys. J. **A6**, 415 (1999).
- [25] R. Venugopalan and M. Prakash, Nucl. Phys. **A546**, 718 (1992).
- [26] H. Stöcker and W. Greiner, Phys. Rep **137**, 277 (1986) and references therein.
- [27] L.D. Landau and E.M. Lifschitz, *Fluid Mechanics*, 2nd Edition (Butterworth and Heine-  
mann,1987), pg. 2.
- [28] E. Schnederman, J. Sollfrank, U.Heinz, Phys. Rev. **C48**, 2462 (1993).
- [29] STAR Collaboration, C. Adler *et al.* , Phys. Rev. Lett. **87**, 182301 (2001).
- [30] P. Huovinen, M. Belkacem, P.J. Ellis and J.I. Kapusta, nucl-th/0112083.